

Nonlinear diffusion in relativistic heavy-ion collisions?

A. Simon and G. Wolschin*

*Institut für Theoretische Physik der Universität Heidelberg,
Philosophenweg 16, D-69120 Heidelberg, Germany, EU*

(Dated: July 26, 2019)

The nonequilibrium-statistical Relativistic Diffusion Model (RDM) is investigated in a generalized version with a nonlinear diffusion term. Broad rapidity distributions encountered in relativistic heavy-ion data for stopping and particle production at SPS and RHIC energies are interpreted as being due to diffusion and collective expansion. Nonextensive statistics has been proposed to account for both effects simultaneously through a nonlinear diffusion term in the Fokker-Planck equation. We show in numerical solutions that this approach fails when compared to data, whereas the linear model with adjusted diffusion coefficient represents the data.

PACS numbers: 25.75.-q, 24.10.Jv, 24.60.-k

I. INTRODUCTION

In relativistic heavy-ion collisions, the observation of very broad rapidity spectra of produced particles and in stopping (proton minus antiproton distributions) as compared to thermal model predictions is a generic feature. It can be interpreted as being due to the interplay of nonequilibrium-statistical processes which cause heating, and collective expansion of the system.

Within the macroscopic relativistic diffusion model (RDM, [1]) two collectively expanding sources provide descriptions of stopping data at centre-of-mass energies up to 200 GeV per particle pair, which is the maximum energy reached at the Relativistic Heavy Ion Collider RHIC. Three sources are required for charged-hadron production [2], yielding predictions up to LHC energies of 5 TeV. The model is based on Boltzmann statistics, a linear Fokker-Planck equation (FPE) for the variables rapidity $y = 1/2 \ln[(E + p_{\parallel})/(E - p_{\parallel})]$ and time t , with a diffusion coefficient D that is adjusted to the data.

As an alternative, it has been proposed to interpret the broad stopping distributions using nonextensive statistics [3–5], with a nonlinear diffusion term in the Fokker-Planck equation. The idea is to account simultaneously for both thermal and collective expansion effects through a nonextensivity coefficient q as proposed by Tsallis et al. [6] that enters the transport equation as an exponent $2-q$ in the diffusion term [3–6]. It is supposed to account for long-range correlations that cause collective expansion, and considered to be a fundamental property of the system like the temperature T . It goes along with a modified definition of the system's entropy [6] which is, however, controversial [7, 8]. This approach would have the additional reward that the Einstein relation between drift and diffusion coefficient that is valid in a linear theory at equilibrium, and approximately valid close to equilibrium, could be maintained [3].

Indeed such a procedure provides fits [3, 4] to stopping data in PbPb and AuAu collisions at energies reached at the Super Proton Synchrotron (SPS) and the Relativistic Heavy Ion Collider (RHIC) with values $1 < q < 4/3$. (No stopping distributions will be available in the foreseeable future from the Large Hadron Collider LHC due to the lack of a suitable forward spectrometer). However, the solutions of the nonlinear FPE are obtained by starting from the stationary solution as proposed in [6], and then solving the problem for time-dependent temperatures $T(t)$ and mean values of the rapidity $y_m(t)$.

It is the aim of this work to solve the nonlinear FPE directly with realistic physical initial conditions that are disconnected from the stationary solution. We shall use several independent numerical schemes, but without a pre-determined form of the solutions, and then try to fit the measured stopping distributions at SPS and RHIC energies with a value of $q > 1$.

Some relevant model ingredients for the linear and nonlinear cases are summarized in the next two sections. The numerical calculations are prepared and tested in the subsequent section. In particular, their implementation is compared to the exact solution of the linear case, and to a specific exact solution of the nonlinear case found by Borland et al. [9]. The latter provides a particularly precise test of the numerical methods, but it is not useful for a solution of the physical problem with δ -function initial conditions at the beam rapidities. We also compare three completely independent solution schemes for the nonlinear problem with each other.

In the final section, we apply the numerical solution of the nonlinear FPE to the calculation of net-proton distributions in PbPb and AuAu collisions at SPS and RHIC energies, and show that it is not possible to fit the data using solutions of the nonlinear FPE with values of the nonextensivity coefficient $q \leq 1.5$. Instead we fit the data in the linear model with an adjusted diffusion coefficient to account for both, nonequilibrium thermal broadening, and collective expansion. The results are then briefly summarized.

* g.wolschin@thphys.uni-heidelberg.de

II. BASIC CONSIDERATIONS

In relativistic heavy-ion collisions, the relevant observable in stopping and particle production is the Lorentz-invariant cross section

$$E \frac{d^3N}{dp^3} = \frac{d^2N}{2\pi p_T dp_T dy} = \frac{d^2N}{2\pi m_T dm_T dy} \quad (1)$$

with the energy $E = m_T \cosh(y)$, the transverse momentum $p_T = \sqrt{p_x^2 + p_y^2}$, the transverse mass $m_T = \sqrt{m^2 + p_T^2}$, and the rapidity y . In this work we concentrate on rapidity distributions of protons minus produced antiprotons, which are indicative of the stopping process as described phenomenologically in a relativistic diffusion model (RDM) [1, 2], or in a QCD-based approach [10]. The rapidity distribution is then obtained by integrating over the transverse mass

$$\frac{dN}{dy}(y, t) = C \int m_T E \frac{d^3N}{dp^3} dm_T, \quad (2)$$

with a normalization constant C that depends on the number of participants at a given centrality. We rely on Boltzmann-Gibbs statistics and hence, adopt the Boltzmann distribution as the thermodynamic equilibrium distribution at temperature T

$$\begin{aligned} E \frac{d^3N}{dp^3} \Big|_{\text{eq}} &\propto E \exp(-E/T) \\ &\equiv m_T \cosh(y) \exp(-m_T \cosh(y)/T). \end{aligned} \quad (3)$$

In thermodynamics one makes the distinction between extensive and intensive properties. Intensive properties do not depend on the size of the system or the amount of mass inside the system. These are for example the temperature or the mass density. Extensive properties on the other hand are proportional to the mass and increase as the size of the system increases. Typical examples are the volume and the mass itself.

In statistical physics, the entropy is also extensive: The Boltzmann-Gibbs' definition of the entropy is $S = -k_B \sum_{i=1}^n p_i \ln(p_i)$, where p_i equals the probability of the system to be in the microstate i . In the case of equal probabilities and a total number of states Ω it follows that $p_i = p = \frac{1}{\Omega}$ and (with $k_B \equiv 1$)

$$\begin{aligned} S &= - \sum_{i=1}^n \frac{1}{\Omega} \ln\left(\frac{1}{\Omega}\right) = - \sum_{i=1}^n \frac{1}{\Omega} (0 - \ln(\Omega)) \\ &= \ln(\Omega), \end{aligned} \quad (5)$$

which is the well-known expression for the entropy. To show its extensivity take two equal systems A and B which do not interact. The number of available microstates in the combined system is equal to the product of the ones in the individual systems as they do not interact,

$$\Omega(A+B) = \Omega(A) \Omega(B). \quad (6)$$

Inserting this into the definition of entropy one gets

$$\begin{aligned} S(A+B) &= \ln(\Omega(A+B)) \\ &= S(A) + S(B) \end{aligned} \quad (7)$$

Hence, the Boltzmann-Gibbs entropy is an extensive property of the system.

Although classical thermodynamics is a very successful theory, discrepancies with respect to data can arise. This is particularly relevant in case of nonequilibrium systems, such as relativistic heavy-ion collisions. However, statistical mechanics is then still built upon the principle that the information I is minimized with constraints that are appropriate for the given physical situation, and the entropy is uniquely defined as $S = -k_B I$.

Nevertheless, different concepts of entropy have been developed for nonequilibrium systems. In particular, Tsallis has proposed to resort to nonextensive statistics [6, 11] where the entropy does not fulfil Eq. (7) but is instead given by

$$\begin{aligned} S_q &= \langle \ln_q \frac{1}{p_i} \rangle = \sum p_i \ln_q \frac{1}{p_i} \\ &= \frac{\sum p_i - \sum p_i^q}{q-1} = \frac{1 - \sum p_i^q}{q-1} \end{aligned} \quad (8)$$

with the entropic index $q \in \mathbb{R}$. Here the logarithm which causes the additivity of the entropy has been replaced by the non-additive q -logarithm $\ln_q(x)$ such that $S_q(A+B) = S_q(A) + S_q(B) + (1-q)S_q(A)S_q(B)$, and q measures the degree of nonextensivity. The inverse of the q -log is the q -exponential e_q^x that solves the differential equation $dy/dx = y^q$ through

$$y = [1 + (1-q)x]^{1/(1-q)} \equiv e_q^x. \quad (9)$$

In the limit $q \rightarrow 1$, S_q is equal to S because

$$\begin{aligned} p_i^q &= e^{\ln(p_i)^q} = e^{\ln(p_i)^{q-1} \ln(p_i)} \\ &= e^{(q-1)\ln(p_i)} p_i = p_i [1 + (q-1)\ln(p_i)] + O(\|q-1\|^2) \end{aligned} \quad (10)$$

provided the last term in Eq. (10) is neglected,

$$\begin{aligned} S_{q \rightarrow 1} &= \frac{1 - \sum p_i [1 + (q-1)\ln(p_i)]}{q-1} \\ &= \frac{1 - \sum p_i + (q-1) \sum p_i \ln p_i}{q-1} \\ &= \sum p_i \ln p_i = S. \end{aligned} \quad (11)$$

There is, however, no clearly defined physical process that would warrant a generalization from S to S_q , and no theory available to calculate the nonextensivity exponent q from first principles. It can still successfully be used as an additional fit parameter, in particular for p_T -distributions in pp and AA collisions at relativistic energies which show a transition from exponential to power-law behaviour that the e_q^x -function properly describes with $q \in (1, 1.5)$. From a more fundamental point of view, the approach is controversial [7, 8].

III. FOKKER-PLANCK EQUATION

The general form of the linear Fokker-Planck equation (FPE) is [12]

$$\frac{\partial}{\partial t}W(x,t) = \frac{\partial}{\partial x}(-A(x,t)W(x,t)) + \frac{\partial^2}{\partial x^2}(D(x,t)W(x,t)) \quad (12)$$

where A is called the drift coefficient and D the diffusion coefficient. It can also be written as a continuity equation for the probability distribution W as

$$\frac{\partial}{\partial t}W + \frac{\partial}{\partial x}J = 0, \quad (13)$$

with $J = \left[A(x,t) - \frac{\partial}{\partial x}D(x,t) \right] W$, which is interpreted as a probability current [12]. Even for coefficients A and D that are not time dependent it is generally difficult, if not impossible to find analytical solutions. Two important examples where solutions do exist are for $A(x,t) = 0$ and $D(x,t) = D$ (Wiener process) or $A(x,t) = -\alpha x$ and $D(x,t) = D$ (Uhlenbeck-Ornstein process). For more complicated problems, especially nonlinear ones, numerical methods are employed.

In the relativistic diffusion model the time evolution of the rapidity spectra has been modeled by a FPE. At first a linear drift ansatz has been tested [1]. The stationary solution in such a case is determined as

$$\frac{\partial}{\partial x} \left[xW + \frac{\partial}{\partial x}W \right] = 0 \implies \frac{\partial W}{\partial x} = -xW + C, \quad (14)$$

C has to be equal to zero because otherwise $W < 0$.

$$\int \frac{1}{W} dW = \int -x dx \implies \ln W = -\frac{1}{2}x^2 + \text{const} \\ \implies W \propto e^{-\frac{1}{2}x^2}. \quad (15)$$

This does not correspond to the equilibrium distribution form Eq. (3) and therefore another drift term is needed. We see from the above calculation that a stationary solution $W \propto e^{-V(x)}$ results from a drift term $V'(x)$. Setting $A = \sinh(x)$ we get the desired stationary solution. This drift term has also been investigated in [13] and the result was again that the fluctuation-dissipation theorem is violated: The diffusion is too small to account for the experimental data. Such a result is not surprising since the theorem should be valid only at or near equilibrium, which is not the case in relativistic heavy-ion collisions, at least not for longitudinal variables such as the rapidity.

The canonical interpretation of this result is that collective expansion occurs in the quark-gluon-plasma phase and increases the width. One way to match the observation is to simply increase the diffusion coefficient, attributing the effect to collective expansion [13, 14]. Another possibility is to change the underlying equation to account for the 'anomalous' diffusion [3–5]. In the latter

approach which we want to test here, one extends the model to a nonlinear FPE (NLFPE)

$$\frac{\partial}{\partial t}W^\mu(x,t) = \frac{\partial}{\partial x}(-A(x,t)W^\mu(x,t)) \\ + \frac{\partial^2}{\partial x^2}(D(x,t)W^\nu(x,t)). \quad (16)$$

Tsallis and Bukman have shown in [6] that the result of maximizing the entropic form

$$S_q[p] = \frac{1 - \int du [p(u)]^q}{q - 1}, \quad (17)$$

leads to the function

$$p_q(x,t) = \frac{\left\{ 1 - \beta(t)(1-q) [x - x_m(t)]^2 \right\}^{1/(1-q)}}{Z_q(t)}. \quad (18)$$

When assuming a linear drift term A in Eq. (16) this function $p_q(x,t)$ solves the partial differential equation (PDE) with additional conditions on $\beta(t)$, $x_m(t)$ and $Z_q(t)$, and one can identify q from the entropic form with the exponents μ and ν of the NLFPE Eq. (16) as $q = 1 + \mu - \nu$ [6].

This identification is actually only justified in the case of linear drift, which is not the one we will use because the Boltzmann equilibrium form requires a sinh-drift. It was also shown in [6] that the norm is only conserved for $\mu = 1$ and since we model a probability distribution we will set μ to one. Differentiating the diffusion term once we get

$$\frac{\partial^2}{\partial x^2} [W^{2-q}] = \frac{\partial}{\partial x} \left[(2-q)W^{1-q} \frac{\partial W}{\partial x} \right]. \quad (19)$$

This means that we can view the nonlinearity in the exponent as ordinary diffusion extended by a nonlinear diffusion coefficient, namely $D'(W) = D(2-q)W^{1-q}$. It is visualised in Fig. 1. For function values of less than one diffusion is increased and for values larger than one it is suppressed. This leads to thinner peaks and faster diffusion at the tails.

The width that we used for the simulation ($\sigma = 0.1$), represented by the middle curve in Fig. 1, peaks at $y = 4$. This results in diffusion coefficients of 0.5 and 0.75, depending on the q . At the tails the diffusion amplification peaks at a factor of 5 or 6 before the distribution functions get negligibly small. The factor $(2-q)$ further weakens the diffusion as q is always greater than one.

IV. NUMERICAL CALCULATIONS

A. General procedure

To arrive at a usable form for the computer we transform the equation into its dimensionless version by introducing a new time-scale t_c resulting in the time variable

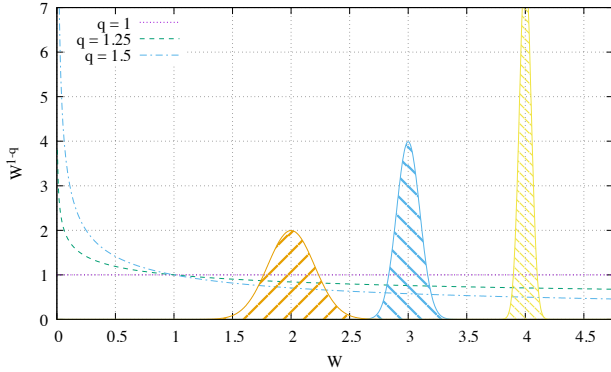


Figure 1. (Color online) Comparison of the diffusion nonlinearity W^{1-q} for different q values. The coefficient is variable for $q > 1$ and depends on the size of the probability distribution itself. To get an idea about the size of (normalized) probability distributions we also plotted Gauss curves with $\sigma = 0.2, 0.1, 0.05$. The height of the Gauss curve then corresponds to W .

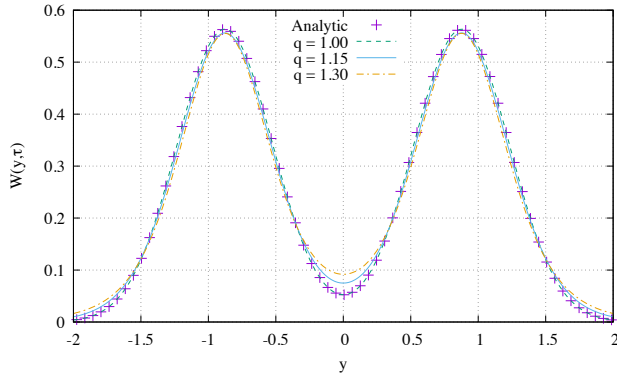


Figure 2. (Color online) Comparison of the analytic linear drift model (crosses) and the corresponding numerical solution ($q=1$, dashed curve). The numerical solutions for two different values of q are also shown (solid for $q=1.15$, dash-dotted for $q=1.3$). The parameters are $\gamma = 0.137$, $y_0 = 2.9$, $\sigma = 0.1$, $\tau = 1.2$.

$\tau = t/t_c$. It follows that $\frac{\partial}{\partial t} = \frac{\partial}{\partial \tau} t_c^{-1}$ and further

$$\frac{\partial f}{\partial \tau} = t_c A \frac{\partial}{\partial y} [\sinh(y) f(y, t)] + t_c D \frac{\partial^2}{\partial y^2} [f(y, t)^{2-q}]. \quad (20)$$

Since $A = \frac{m_T D}{T}$ we set $t_c = \frac{T}{m_T D} = A^{-1}$. The result is the dimensionless Eq. (21) depending only on the ratio $\gamma = \frac{T}{m_T}$ of temperature T and transverse mass m_T which is a measure of the strength of the diffusion.

$$\frac{\partial f}{\partial \tau} = \frac{\partial}{\partial y} [\sinh(y) f(y, t)] + \gamma \frac{\partial^2}{\partial y^2} [f(y, t)^{2-q}]. \quad (21)$$

To get physical values for the drift and diffusion coefficients one has to specify a time scale (or the other way round). Considering that it is only the drift term that is

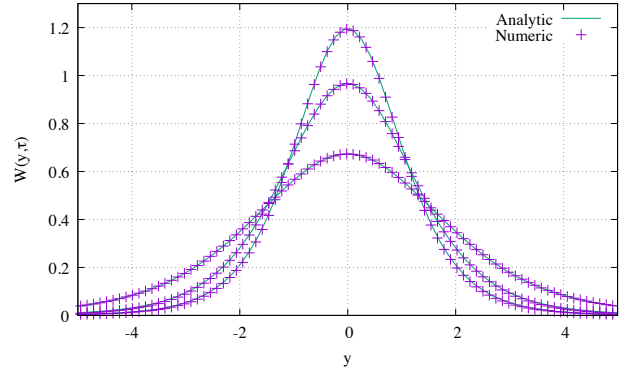


Figure 3. (Color online) Comparison of the analytical (solid curves) and numerical (crosses) solutions for $q = 1.3$ at different dimensionless times $\tau = 0.2, 0.5, 0.8$. (Top to bottom at $y = 0$).

responsible for determining the peak position we are free to choose the time τ such that the peak position of the experimental data is reproduced. This leaves as free parameters the diffusion strength γ and the non-extensivity parameter q .

We calculated the solution using two different methods, in order to gain insight about the accuracy. The more straightforward one was using MATLAB's integration routines for solving parabolic-elliptic PDEs. The second, more elaborate method, was implementing it in a Finite-Element-Method framework (FEM) (DUNE [15] and FEniCS [16]).

To make use of the FEM we have to convert our PDE into the so called weak formulation which reformulates the problem as an integral equation. This is done by integrating the lhs of Eq. (21) over the whole domain $\Omega \subset \mathbb{R}$ and multiplying it by a test function $g(y)$ that vanishes on the boundary $\partial\Omega$,

$$\int_{\Omega} dy \left\{ g(y) \frac{\partial}{\partial y} \left[\sinh(y) f(y, t) + \gamma \frac{\partial}{\partial y} f(y, t)^{2-q} \right] \right\}. \quad (22)$$

Integrating this by parts we get

$$\left[g(y) \left\{ \sinh(y) f(y, t) + \gamma \frac{\partial}{\partial y} f(y, t)^{2-q} \right\} \right] \Big|_{\partial\Omega} - \int_{\Omega} dy \left\{ \frac{dg}{dy} \left[\sinh(y) f(y, t) + \gamma \frac{\partial}{\partial y} f(y, t)^{2-q} \right] \right\}. \quad (23)$$

The first line in Eq. (23) vanishes because of g and the second line contains only first derivatives. To approximate the time derivative in Eq. (22) (RHS) we use the Backward-Euler scheme

$$\frac{\partial f(t_n)}{\partial t} = \frac{f(t_n) - f(t_{n-1})}{\Delta t} + O(\|\Delta t^2\|). \quad (24)$$

For both methods the chain rule is used to write $\frac{\partial}{\partial x} f^{2-q}$ as $(2-q)f^{1-q} \frac{\partial}{\partial x} f$. Because we analyze cases for $q > 0$

we have to take care of the singularity at $f = 0$. To get around this issue we add a small constant to the argument stabilizing the computation: $(f + \epsilon)^{1-q}$. In MATLAB we use the routine `pdepe` to integrate the equation. It is suited for parabolic-elliptic problems and we could directly insert the PDE without modifying it.

To compare the simulation to experimental data we have to insert relevant values for T , m_T and the initial conditions, most importantly y_0 . The value of the beam rapidity y_0 is determined by the center-of-mass energy per nucleon pair as $y_0 = \ln(\sqrt{s_{NN}}/m_p)$. Two Gaussian distributions centered at $\pm y_0$ with a small width σ that corresponds to the Fermi motion represent the incoming ions before the collision. The exact value of σ does not have a large effect on the time evolution [13]; here we use a value of 0.1.

For the temperature we take the critical value 160 MeV for the transition between hadronic matter and quark-gluon-plasma. The actual freeze-out temperature is smaller ($T = 118 \pm 5$ MeV for PbPb at SPS energies [17]); overestimating the temperature will increase the diffusion. For 17.2 GeV PbPb, the transverse mass is taken to be $m_T = 1.17$ GeV as the average transverse momentum p_T is around 0.7 GeV [17]. The dimensionless diffusion strength γ is thus 0.137. Corresponding values for 200 GeV AuAu will be given later. The results are then transformed to a rapidity distribution by [13]

$$\begin{aligned} \frac{dN}{dy}(y, t) &= C \int_{m_p}^{\infty} m_T^2 \cosh(y) f(y, t) dm_T \\ &\approx \tilde{C} \langle m_T^2 \rangle \cosh(y) f(y, t). \end{aligned} \quad (25)$$

The constant \tilde{C} is chosen such that the total number of particles for 0%-5% centrality corresponds to the number of participant protons in this centrality bin.

B. Tests of the numerical implementation

In order to check the numerical implementation we compare it to analytically solvable problems. At first we consider the linear drift model and compare the numerical solution for different values of q , first for $q = 1$ (where both should be the same) and then for other values of q , Fig. 2. This gives us a first idea about the impact of the non-linearity parameter on the evolution.

The numerical result for $q = 1$ is identical with the analytical solution, which validates the numerical method. By increasing q the peaks are slightly smeared out, giving an overall flatter shape than before. This is expected since a larger diffusion coefficient will spread out the profile faster.

As the next problem we take the one solved analytically by Borland et al. in [9]

$$\frac{\partial f}{\partial t} = \frac{\partial}{\partial y} (yf) + \frac{\partial^2}{\partial y^2} f^{2-q}. \quad (26)$$

The results are displayed in Fig. 3.

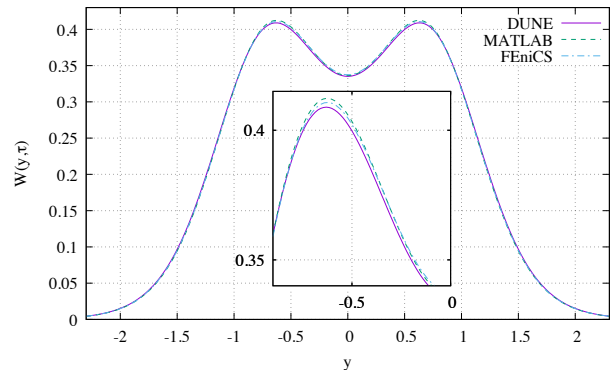


Figure 4. (Color online) Comparison of the three numerical solution methods for $\tau = 1$ and $\gamma = 0.137$.

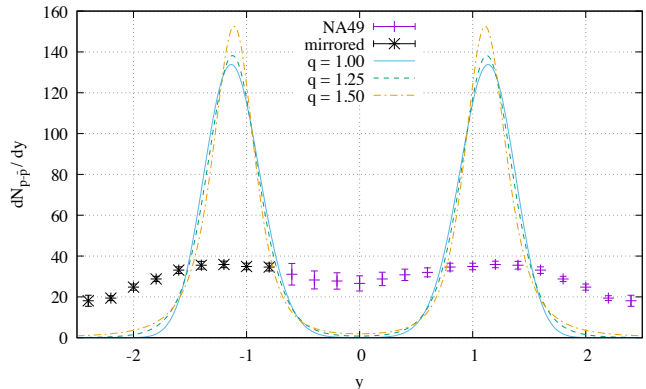


Figure 5. (Color online) Numerical solutions of the nonlinear FPE for central PbPb at 17.2 GeV with three different values of $q \in [1, 1.5]$, and NA49 data [17].

The solution assumes that the initial condition is functionally equal to the stationary solution, except for time dependent coefficients. In particular, both the stationary solution, and the initial conditions are centered at $y = 0$, which is essential to obtain the analytical solution of the time-dependent problem. It is thus not useful for our physical situation with initial conditions that are adapted to the heavy-ion collision case, but we get the possibility to compare the anomalous diffusion to an analytical solution.

In the case of a heavy-ion collision, the initial distributions are both off-center at the values of the beam rapidities, whereas the stationary solution that is obtained for $t \rightarrow \infty$ is centered at rapidity $y = 0$ and hence, the Borland et al. analytical solution can not be used. Instead, the time-dependent solution in the heavy-ion case drifts towards midrapidity, and hence, the time-dependent equation must be solved with the beam rapidities $y_{\text{beam}} = \pm y_0$ defining the initial conditions (δ -functions, or Gaussians with a width that is determined by the Fermi motion).

The agreement between analytical and numerical solution in the case of initial conditions that are centered

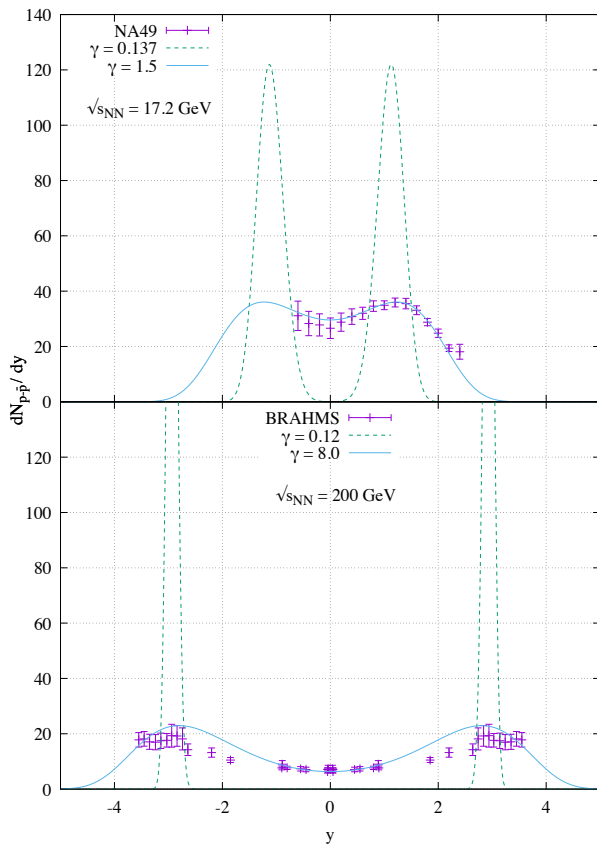


Figure 6. (Color online) Comparison of the linear model without (dashed) and with (solid) adjusted diffusion term with NA49 data for 0-5% central PbPb at $\sqrt{s_{NN}} = 17.2$ GeV [17], upper frame, and with BRAHMS data for central AuAu at $\sqrt{s_{NN}} = 200$ GeV [18], lower frame. The values of the dimensionless diffusion strengths are $\gamma = 0.137$ and 0.12 from the dissipation-fluctuation theorem, whereas $\gamma = 1.5$ and 8.0 are adjusted to the SPS and the RHIC data, respectively, and account also for collective expansion. The values of the interaction time have been adjusted in both cases. A numerical solution of the nonlinear diffusion equation with $q > 1$ does not fit the data for any value of γ and time.

at $y = 0$ further supports the correctness of the implementation. We have now three numerical schemes at our disposal to calculate the evolution. Since they are based upon two different mathematical methods (Finite Elements and Finite Differences) it is unlikely that a hypothetical programming error occurred in all of them. Having this in mind we simulated the full PDE using each of the packages and compared the results. The time evolution of two Gaussian peaks with $y_0 = 2.9$ and $\sigma = 0.1$ at the time $\tau = 1$ is shown in Fig. 4.

The relative difference between the solutions using the three numerical schemes is around 1% and mostly concentrated at the peaks. Possible origins of the slight discrepancies are the different step sizes used in each discretisation and the basis functions used in the FEM interpolation. In any case the differences are very small,

from which we conclude that the calculations are correct. Since further data analysis is easiest in MATLAB, we use it in the following calculations.

V. COMPARISON OF NUMERICAL RESULTS AND EXPERIMENTAL DATA

The results of the calculation for different values of q are shown in Fig. 5 for PbPb at 17.2 GeV. While a larger q does broaden the distribution, the effect is by far too small to come close to the experimental results.

In order to reproduce the measured data for PbPb we have to adopt a diffusion strength of around 1.5 while the one predicted by the fluctuation-dissipation theorem is around 0.137, the difference being a factor 11, see the upper frame of Fig. 6. As we mentioned earlier and as can be seen in Fig. 1, such a large enhancement in the required broadening cannot be compensated by the proposed nonlinearity due to q -statistics.

The comparison with AuAu stopping data at the maximum energy of 200 GeV reached at RHIC shows that here the discrepancy between the diffusion strength from the fluctuation-dissipation theorem ($\gamma = 0.12$) and the one required to fit the data ($\gamma = 8$) with an adjusted value of time is even larger, see lower frame of Fig. 6. This means that introducing a nonlinearity into the diffusion term cannot account for the observed rapidity spectra at SPS and RHIC energies. Since the widths are too narrow there has to be an additional expansion process that takes place during the reaction that can not be accounted for by q -statistics. This result is in obvious contrast to the findings of [3-5], where an approximate solution of Eq. (21) had been used.

We have also solved the nonlinear diffusion equation separately for initial conditions centered at $y_{\text{beam}} = +y_0$, and at $y_{\text{beam}} = -y_0$ to assess how much the superposition principle is violated in the nonlinear case. Adding the results shows that the difference with respect to the full numerical solution remains, however, below 5% at midrapidity.

As the numerical solution of the nonlinear Eq. (21) does not explain the experimental data, we return to the model with linear diffusion $q \equiv 1$, and the drift term imposed by the stationary solution [13]. By fitting experimental data to this model we can find physical values for the drift and diffusion coefficients in stopping using the two data sets from NA49 [17] at $\sqrt{s_{NN}} = 17.2$ GeV with beam rapidity $y_{\text{beam}} = \pm 2.91$, and BRAHMS [18] at $\sqrt{s_{NN}} = 200$ GeV with $y_{\text{beam}} = \pm 5.36$ in central collisions of PbPb and AuAu, respectively. With an interaction time of 8 fm/c, we obtain the results shown in Table I. Corresponding values with energy-dependent interaction times had been obtained in [13].

The failure to interpret the broad rapidity distributions observed in the stopping process of relativistic heavy-ion collisions within q -statistics refers specifically to the solution of the nonlinear Fokker-Planck Eq. (16) which arises

System	$\sqrt{s_{NN}}$ (GeV)	A (10^{24} s^{-1})	D (10^{24} s^{-1})
PbPb	17.2	4.06	6.67
AuAu	200	5.17	53.4

Table I. Fitted values for the drift and diffusion coefficients in the case of normal diffusion

within nonextensive statistics [6, 11]. Among the abundant publications that compare q -statistics with data in particular for p_T -distributions (e.g. [19–21]), but also for rapidity distributions ([20]), only few such as [3, 4] refer to an explicit – but approximate – solution of the basic nonlinear FPE. The result that was derived there makes use of the form of the stationary solution, replacing temperature and mean rapidity by time-dependent quantities. The outcome of this procedure does not agree with our numerical results for the explicit solution of the nonlinear FPE.

VI. CONCLUSION

We have solved a Fokker-Planck equation with non-linear diffusion term numerically with the aim to describe rapidity distributions for stopping in relativistic heavy-ion collisions at energies reached at the Super Proton Synchrotron and the Relativistic Heavy Ion Collider. The use of three different numerical methods with co-

inciding outcome and various cross checks with exact analytical results ensure the accuracy of the numerical calculations.

The discrepancies between the linear diffusion model with dissipation-fluctuation theorem and the experimental data regarding the widths of the rapidity distributions for stopping [14] could, however, not be resolved by introducing the entropy function of non-extensive q -statistics and a corresponding nonlinear diffusion term in the Fokker-Planck equation.

This is in contrast to the work of Lavagno et al. [3–5] where the same problem was treated with the conclusion that the experimental data were perfectly reproduced for specific values of $q \in (1, 1.5)$. In their work, the nonlinear equation had been solved using the form of the stationary solution as an ansatz for the numerical integration, which could be a possible origin of the difference in the results.

When comparing with data, we therefore start from the unmodified equation with a linear diffusion term as in Boltzmann statistics, and determine values of the diffusion coefficient that are necessary to reproduce the measured data, thus accounting phenomenologically for both nonequilibrium thermal processes and collective expansion without a nonlinear diffusion term.

ACKNOWLEDGMENTS

We are grateful to Andreas Mielke for discussions and remarks.

-
- [1] G. Wolschin, Eur. Phys. J. A **5**, 85 (1999).
 - [2] G. Wolschin, Phys. Rev. C **94**, 024911 (2016).
 - [3] A. Lavagno, Physica A **305**, 238 (2002).
 - [4] W. M. Alberico, P. Czerskic, A. Lavagno, M. Nardi, and V. Somà, Physica A **387**, 467 (2008).
 - [5] W. M. Alberico and A. Lavagno, Eur. Phys. J. A **40**, 313 (2009).
 - [6] C. Tsallis and D. J. Bukman, Phys. Rev. E **54**, R2197 (1996).
 - [7] M. Nauenberg, Phys. Rev. E **67**, 036114 (2003).
 - [8] R. Balian and M. Nauenberg, Europhys. News **37**, 9 (2006).
 - [9] L. Borland, F. Pennini, A. R. Plastino, and A. Plastino, Eur. Phys. J. B **12**, 285 (1999).
 - [10] Y. Mehtar-Tani and G. Wolschin, Phys. Rev. Lett. **102**, 182301 (2009).
 - [11] C. Tsallis, J. Stat. Phys. **52**, 479 (1988).
 - [12] H. Risken and T. Frank, The Fokker-Planck equation (Springer, 1996).
 - [13] F. Forndran and G. Wolschin, Eur. Phys. J. A **53**, 37 (2017).
 - [14] G. Wolschin, Europhys. Lett. **47**, 30 (1999).
 - [15] P. Bastian, F. Heimann, and S. Marnach, Kybernetika **46**, 294 (2010).
 - [16] M. S. Alnæs *et al.*, Archive of Num. Software **3**, 9 (2015).
 - [17] H. Appelshäuser *et al.*, Phys. Rev. Lett. **82**, 2471 (1999).
 - [18] I. G. Bearden *et al.*, Phys. Rev. Lett. **93**, 102301 (2004).
 - [19] G. Wilk and Z. Włodarczyk, Eur. Phys. J. A **40**, 299 (2009).
 - [20] L. Marques, J. Cleymans, and A. Deppman, Phys. Rev. D **91**, 054025 (2015).
 - [21] C.-Y. Wong, G. Wilk, L. J. L. Cirto, and C. Tsallis, Phys. Rev. D **91**, 114027 (2015).